Experimental Investigation into Texture Analysis of Machined and 3D printed Surfaces.

M. B. Kiran
Associate Professor,
Department of Mechanical Engineering,
School of Technology,
Pandit Deendayal Energy University,
Gandhinagar, Gujarat, INDIA
MB.Kiran@sot.pdpu.ac.in

Abstract

Texture analysis and evaluation would help in predicting a component's functionality. An attempt has been made in the current research work to explore the texture properties of machined surfaces in detail. Pieces made from milling, shaping, grinding, EDM, and sandblasting processes are used for texture analysis. The method uses a charge-coupled device (CCD) camera connected to the vision system to acquire images for texture analysis. The experimental investigation revealed that texture features extracted from the grey level co-occurrence matrix (GLCM) help study texture features. The experimental investigation revealed that when distance =1, the classification accuracy was less. However, the classification accuracy improved when distance =2, but a further increase in the distance would not significantly improve the classification accuracy. Instead, it would add up to the computational time. Thus, it was concluded that d=2 gave maximum classification accuracy of 96%.

Keywords: Surface Texture, Surface Roughness, Waviness, Form Error, Milled Texture.

1. Introduction

Engineering components are made from various primary and secondary manufacturing processes. Primary processes include casting, forging, rolling, extrusion, etc. Machining is an example of a secondary manufacturing process. Every manufacturing process would produce a unique texture. Thus, the texture created from the milling process would differ from that made from a grinding process. Different engineering applications demand different types of surface textures. The texture of a machined surface would consist of surface irregularities having a shorter wavelength known as 'roughness,' a medium wavelength known as 'waviness,' and a large wavelength known as 'form error.' Every engineering application requires specifying both roughness and texture. Thus, in a component's drawing, mention would be made of roughness and texture. And the measurement of both surface and roughness would be crucial in any component inspection. Also, these measurements would help predict the success of the component when it is put into service. This clearly shows the significance of measuring both the roughness and texture. Many researchers have contributed methods and techniques for assessing both roughness and texture. The most popular method for measuring roughness is by contact measurement method. The contact method would be using a diamond stylus to traverse the surface, which would give accurate results. However, they are slow and can be used in post-process inspection of surfaces. To overcome these limitations, non-contact methods using electro-optical techniques came into being. These methods also give accurate readings, but the plans are not widely used in industries. They are mostly restricted to laboratory environments. Also, the technique is susceptible and cannot be used in industrial environments. An attempt has been made in the current research work to study the tribological properties of different machined surfaces utilizing a vision system.

2. Literature review

Many researchers have been working in the area of texture classification. One of the earliest works on Texture reported was by Julesz (1973). One of the characteristics of image textures is the spatial distribution of grey levels. He used both first-order and second-order statistics to define the image texture. First-order statistics can be computed from the image histograms. He concluded that their second-order statistics could not be identical to discriminate between the two images. These approaches may extract texture features directly from images or sometimes in the spatial frequency

domain (Van Gool et al. 1985). Smith et al. (1994) have extracted the mean and variance of wavelet subbands used for texture classification. Ohanian et al. (1992) have studied texture features such as Markov Random Fields, Gabor multi-channel fields, fractal-based features, and co-occurrence matrix-based features. Grey level co-occurrence matrix (GLCM)-based texture features were proposed by Haralick (1979). The GLCM measures the image properties of the second-order statistics. Many research works successfully used GLCM in classifying manufactured products into Good or defective ([a]Kiran 2021). The research has reported that the texture features derived from GLCM gave perfect classification accuracy. GLCM estimates the image properties related to second-order statistics. The method uses an input image N X N with G gray levels. [b] Kiran (2021) explored product inspection using GLCM. In the study, GLCM was constructed with different distances d=1 and 2. Each space would give four co-occurrence matrices corresponding to 0^0, 45^0, 90^0, and 135^0 respectively. The research study of surfaces made out of milling, shaping, Grinding, EDM, and sandblasting was studied. The classification accuracy was good. The autocorrelation function f(x) (Equation 1) is helpful while assessing the type of texture, such as coarseness or fineness.

$$\rho(x,y) = \frac{\sum_{u=0}^{N}\sum_{v=0}^{N} I(u,v)I(u+x,v+y)}{\sum_{u=0}^{N}\sum_{v=0}^{N} I^2(u,v)} \tag{1}$$

It was observed that the autocorrelation function would drop off slowly in case of coarse textures, whereas it would drop off quickly in case of smooth surfaces. Many researchers have done comparative studies to evaluate the performance of different features (Ojala et al. 1996, Reed et al. 1993). Chang et al. (1993) studied tree-structured wavelet transform for performing texture classification. Manjunath et al. (1995) explored classification schemes using tree-structured, orthogonal, and biorthogonal Gabor Wavelet transform. They have concluded that Gabor Wavelet Transform gave excellent classification accuracy among all the studied techniques. Gabor-based texture features were extracted from the input image (Jain et al. 1991). They concluded that Gabor features have desirable optimality properties.

The global frequency content of the signal is analyzed by using Fourier transform. Introducing spatial dependency into Fourier transform would result in *window Fourier transform*. Window Fourier transform is defined as,

$$F_w(u,\xi) = \int_{-\infty}^{\infty} f(x)w(x-\xi)e^{-j2\pi ux}dx \tag{2}$$

Here, when the window function w(x) becomes, it is called Gabor transform. They defined the Gabor filter as a Sinusoidal wave, having a specific *frequency* and *orientation* (Equation-2)

$$f(x,y) = \exp\left(-\frac{1}{2}\left[\frac{x^2}{\sigma_x^2}+\frac{y^2}{\sigma_y^2}\right]\right)\cos(2\pi u_0 x+\phi) \tag{3}$$

In Equation 3, u_0 and ϕ are the frequency and phase of a sinusoidal wave. σ_x and σ_y are the sizes of the Gaussian envelope in the x and y directions. Texture classification is the process of deciding to which class the texture belongs. Supervised and unsupervised methods do texture classification.

In supervised classification techniques, the number of classes is known in advance. The algorithm tries to assign the test image to a class by using distance metrics (e.g., Euclidean distance). In unsupervised classification, the algorithm attempts to extract the classes and then does the classification.

Farrokhnia (1990) studied texture features of painted surfaces. Texture analysis has been studied extensively using satellite remote sensing images (Rignot et al. 1990). They used image restoration procedures to remove specular noise in the image. They used grey level co-occurrence matrix methods for computing the texture features from the input images.

One research work has reported the analysis of texture features obtained from SAR images (Schistad et al. 1992). They studied water, urban area, agriculture, and other areas. They used GLCM-based texture features and Markov random fields (MRF) to classify these images. They identified a maximum classification error of 25% using fractal-based models. They also reported an error of 6% in MRF images. Du et al. (1990) studied and classified SAR images using Gabor filters. [b]Kiran (2021) studied various machined surfaces- milling, grinding, and EDM for roughness measurements. The research has shown that vision roughness correlated well with the average roughness obtained from stylus instruments. The accuracy and repeatability of the technique were excellent. The study showed that the method could be used in 100% inspection of surfaces.

Kiran (1998) and [a.b]Patel et al. (2020) have investigated surface roughness assessment of machined surfaces using the co-occurrence matrix method. The above paragraphs clearly show that much work on textures analysis is required in surface inspection. More understanding of the area of texture would help deliver quality manufactured products. In this context, the present research assumes special significance.

3. Method

For image acquisition, the present research uses a vision system with a (charge-coupled device) CCD camera. Advanced image processing cards fitted to the vision system would help quickly process acquired images such as image quality enhancement, filtering, edge enhancement, etc. Frame grabber connected to the vision system would help get a digital image. A digital image will have a resolution of 1600 X 1236 pixels. The in-house software developed using C++ would help compute the texture features, analyze, and classify various textures.

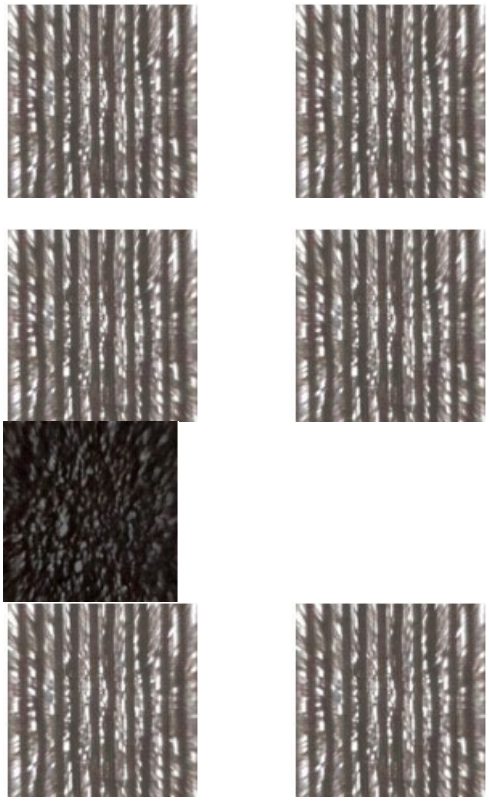

Figure 1. Shaped surface images

Figure 2. EDM surface images

Present research work uses specimens made of various manufacturing processes such as shaping (Figure 1), Electric discharge machining (Figure 2), milling (Figure 3), grinding, Sandblasting (Figure 4), and additive manufacturing. Table 1 shows a digital image of a sample made from Electron Beam melting (3D printing). Specimens are made from various manufacturing processes such as milling, shaping, EDM, sandblasting, and grinding with different machining parameters. The specimen images are classified into the training set and test sets for experimentation. The software

will be trained using the images from the training set. The robustness of the software is tested by using the images from the test set.

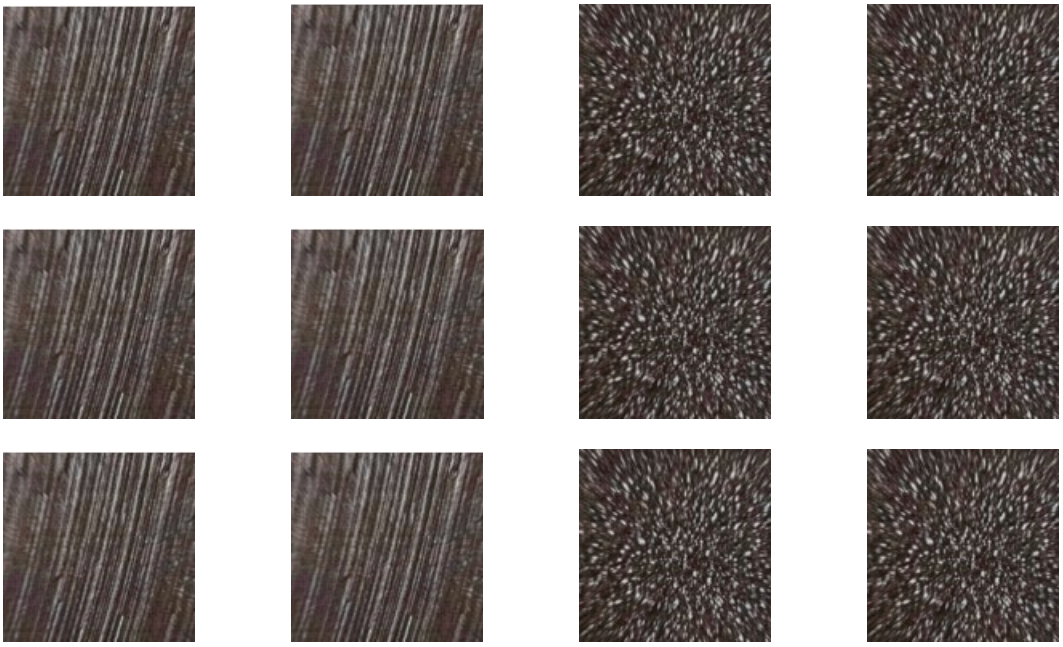

Figure 3. Milled surface images

Figure 4. Sandblasted surface images

Table 1. Digital image of EBM surface image

123	245	267	145	127	234	254
145	143	165	256	223	265	134
147	142	176	189	187	165	190
145	178	189	156	178	179	180
188	176	185	186	143	146	149
154	178	198	245	209	221	267
267	121	143	144	156	165	176
189	145	154	178	187	190	193

4. Results and Discussions

Table 2 shows the co-occurrence matrix of the sandblasted surface image. Table 2(a) shows the 7 X 8 matrix of numbers. Each element in the matrix represents the number of pixels having a particular set of the spatial arrangement of grayscale values within the image at a given distance (d=1) and a given angle (0^0).

Table 2. Co-occurrence matrix of the sandblasted surface image

12	8	4	14	3	34	23
14	13	10	5	2	26	34
17	12	7	19	17	15	19
14	8	19	16	8	7	8
18	17	18	18	14	14	14
14	8	18	24	20	22	27
27	12	4	14	6	16	17
8	14	5	8	18	19	13
17	9	6	12	7	30	21
18	15	12	8	6	24	30
14	14	9	16	14	12	16
11	9	16	14	10	9	9
12	15	17	14	12	12	12
11	9	14	20	22	20	25
20	13	8	16	9	9	15
9	12	9	10	16	7	12

(a) Angle=0^0 (b) Angle=45^0

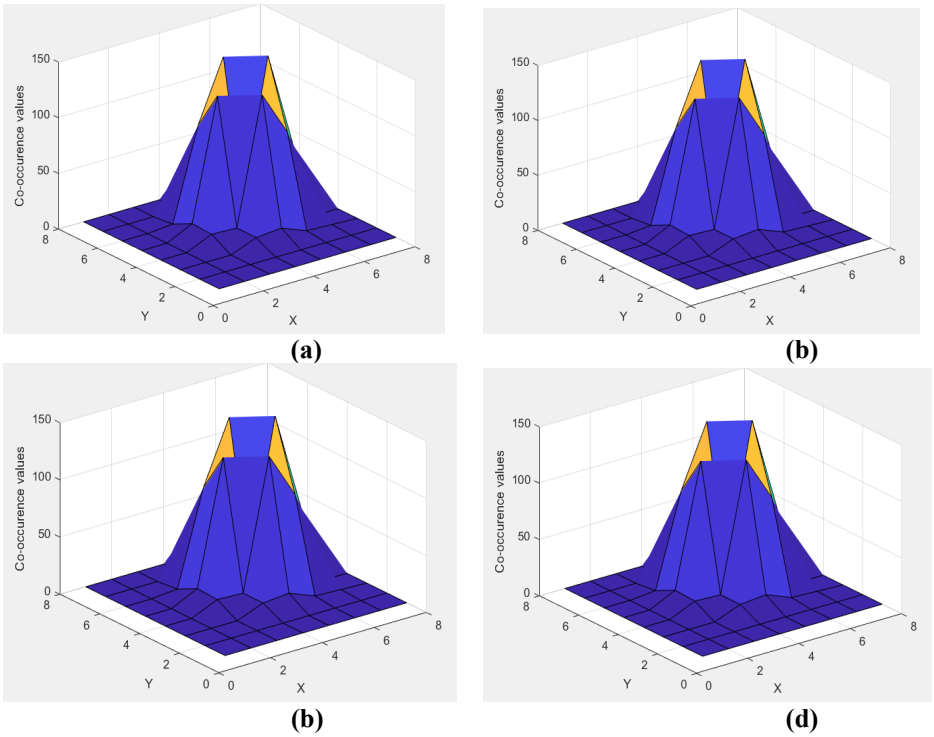

Figure 5. Cooccurrence matrix Plots for 3D Printed surface images, with (d=2) (a) 0^0 (b) 45^0 (c) 90^0 (d) 135^0

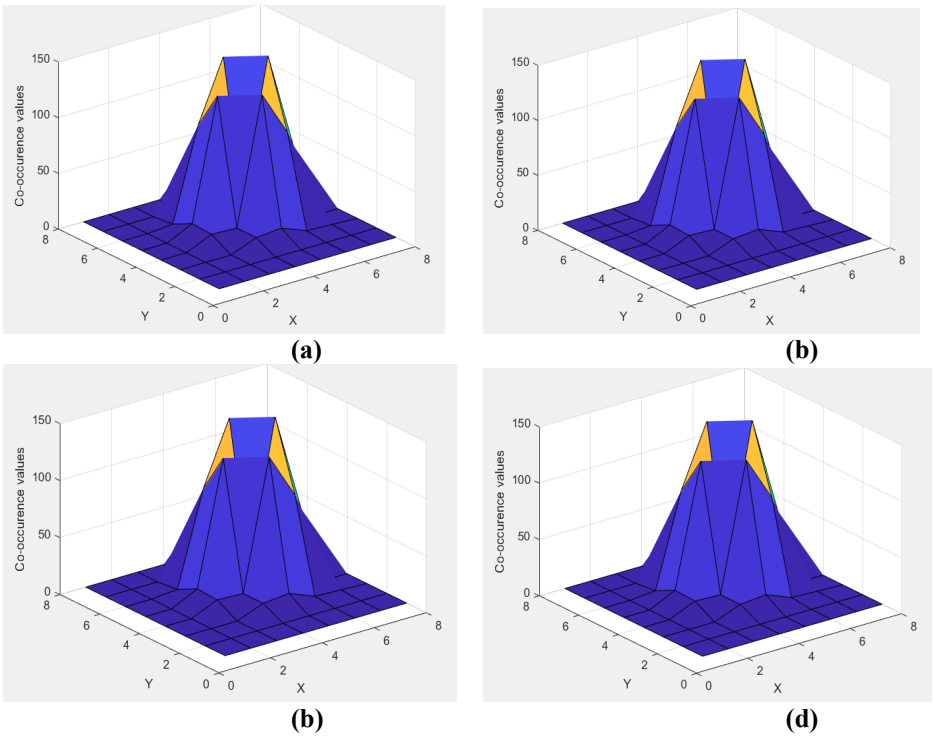

Figure 6. Cooccurrence matrix Plots for sandblasted surface images, with (d=2) (a) 0^0 (b) 45^0 (c) 90^0 (d) 135^0

Table 3. Feature vector (Milling)

Feature No.	1	2	3	4	5	6	7	8	9	10
I	2.96	2.67	2.97	2.85	2.86	2.97	2.97	2.94	2.84	2.94
II	0.19	0.75	0.27	0.35	0.37	0.16	0.15	0.18	0.19	0.16
III	0.95	0.75	0.68	1.07	1.07	0.96	0.97	0.93	0.97	1.07
IV	2.3	2.45	2.26	1.86	2.34	2.37	2.75	2.67	2.54	2.56
V	0.85	0.91	0.55	0.45	0.43	0.57	0.47	0.55	0.56	0.58
VI	1.95	1.37	1.08	0.95	0.93	0.98	1.17	1.05	1.04	0.97
VII	1.86	1.56	1.38	0.99	0.98	1.37	1.69	1.46	1.35	1.34
VIII	57.0	53.9	51.9	58.6	57.9	54.5	51.0	51.7	51.6	53.6
IX	2.31	1.47	0.85	1.37	1.37	0.95	1.38	0.95	0.94	1.37
X	6.50	5.25	4.27	5.78	5.74	5.87	4.87	4.23	5.63	5.77
XI	0.05	0.08	0.98	0.27	0.16	0.05	0.27	0.25	0.25	0.45
XII	0.67	0.57	0.59	0.67	0.86	0.68	0.58	0.56	0.57	0.66

Table 4. Feature vector (Shaping)

Feature No.	1	2	3	4	5	6	7	8	9	10
I	2.93	2.66	2.94	2.83	2.85	2.78	2.96	2.97	2.80	2.55
II	0.14	0.15	0.05	0.38	0.49	0.25	0.19	0.16	0.19	0.25
III	0.86	0.75	0.75	1.07	1.05	0.68	0.79	0.69	0.68	1.14
IV	2.2	2.75	2.26	1.86	2.34	2.49	2.53	2.55	2.79	2.49
V	0.54	0.71	0.67	0.48	0.49	0.48	0.89	0.77	0.63	0.56
VI	1.25	1.08	1.13	0.95	0.97	0.89	1.27	1.27	1.15	0.98
VII	1.36	1.44	1.38	0.79	0.98	1.54	1.57	1.38	1.29	1.59
VIII	53.5	53.4	51.9	58.9	56.8	56.9	51.5	52.6	51.7	52.7
IX	1.81	1.48	0.86	1.65	1.59	0.48	1.42	0.89	0.77	1.25
X	5.56	5.26	4.27	5.69	5.63	5.74	4.49	4.49	5.57	5.55
XI	0.06	0.07	0.09	0.59	0.24	0.23	0.43	0.45	0.26	0.38
XII	0.66	0.56	0.56	0.45	0.56	0.49	0.69	0.37	0.59	0.54

Table 5. Feature vector (EDM)

Feature No.	1	2	3	4	5	6	7	8	9	10
I	2.94	2.66	2.86	2.70	2.57	2.78	2.96	2.97	2.70	2.65
II	0.20	0.15	0.17	0.53	0.37	0.35	0.16	0.17	0.19	0.35
III	0.84	0.54	0.58	1.06	1.07	0.78	0.79	0.79	0.97	1.24
IV	2.1	2.14	2.25	1.68	2.37	2.49	2.63	2.55	2.57	2.39
V	0.54	0.52	0.58	0.46	0.65	0.48	0.69	0.67	0.73	0.47
VI	1.15	1.27	1.23	0.95	0.77	0.95	1.06	1.17	1.04	0.59
VII	1.34	1.44	1.34	0.97	0.65	1.36	1.67	1.28	1.34	1.69
VIII	54.0	53.4	51.5	58.6	57.8	54.7	52.8	50.6	51.6	54.7
IX	1.33	1.44	0.59	1.36	1.37	0.97	1.37	0.79	0.95	1.45
X	5.40	5.24	4.27	5.76	5.73	5.74	4.87	4.59	5.65	5.55
XI	0.04	0.15	0.18	0.27	0.34	0.06	0.27	0.55	0.26	0.98
XII	0.66	0.56	0.56	0.66	0.76	0.69	0.57	0.58	0.57	0.94

Table 6. Feature vector (3D Printing)

Feature No.	1	2	3	4	5	6	7	8	9	10
I	2.97	2.67	2.95	2.70	2.85	2.97	2.78	2.97	2.70	2.75
II	0.13	0.15	0.17	0.63	0.37	0.25	0.27	0.09	0.19	0.05
III	0.75	0.35	0.75	1.24	1.26	0.78	0.69	0.79	0.78	1.07
IV	2.3	2.55	2.26	1.87	2.35	2.37	2.53	2.45	2.49	2.49
V	0.55	0.57	0.55	0.46	0.75	0.68	0.79	0.57	0.33	0.37
VI	1.45	1.27	1.08	0.96	0.87	0.79	1.17	1.17	1.06	0.69
VII	1.76	1.36	1.65	0.69	0.75	1.38	1.57	1.38	1.37	1.59
VIII	57.0	55.6	50.4	57.5	56.8	57.9	50.8	50.6	51.7	52.7
IX	1.61	1.48	0.79	1.65	1.69	0.98	1.42	0.89	0.96	1.35
X	5.80	5.27	4.28	5.49	5.43	5.89	4.87	4.39	5.66	5.55
XI	0.08	0.04	0.06	0.39	0.24	0.13	0.25	0.35	0.37	0.28
XII	0.58	0.57	0.55	0.68	0.46	0.59	0.58	0.77	0.55	0.54

Table 7. Feature vector (Sandblasting)

Feature No.	1	2	3	4	5	6	7	8	9	10
I	2.74	2.66	2.76	2.70	2.67	2.78	2.78	2.78	2.70	2.75
II	0.13	0.04	0.17	0.63	0.19	0.16	0.17	0.17	0.08	0.25
III	0.84	0.58	0.68	1.08	1.16	0.97	0.89	0.97	0.97	1.05
IV	2.02	2.17	2.18	1.85	2.16	2.37	2.63	2.69	2.57	2.57
V	0.54	0.54	0.37	0.47	0.35	0.56	0.59	0.57	0.55	0.56
VI	1.07	1.05	1.05	0.94	0.77	0.97	1.07	1.05	1.08	0.97
VII	1.36	1.46	1.37	0.96	0.95	1.36	1.69	1.45	1.37	1.37
VIII	55.5	53.8	51.5	58.5	57.6	54.6	51.9	50.6	51.7	53.5
IX	1.34	1.44	0.87	1.38	1.37	0.97	1.37	0.79	0.95	1.37
X	5.56	5.26	4.26	5.79	5.83	5.87	4.86	4.59	5.67	5.79
XI	0.06	0.06	0.06	0.39	0.24	0.05	0.26	0.45	0.25	0.47
XII	0.68	0.57	0.56	0.75	0.56	0.68	0.58	0.67	0.57	0.67

Table 8. Classification Experiment (with d=1)

Training							
M	**S**	**G**	**EDM**	**SB**	**TP**	**Accuracy**	**Classified as**
150						**100%**	M
	150					**100%**	S
		150				**100%**	G
			150			**100%**	EDM
				150		**100%**	SB
					150	**100%**	TP

Testing							
M	**S**	**G**	**EDM**	**SB**	**TP**	**Accuracy**	**Classified as**
141	**2**	**2**	**4**	**1**		**94%**	M
	140	**2**	**3**	**2**	**2**	**93.33%**	S
		142	**2**	**1**	**5**	**94.66%**	G
			143	**5**	**2**	**95.33%**	EDM
			1	**142**	**4**	**94.66%**	SB
				6	**144**	**96%**	TP

Note: Milling (M), Shaping (S), Grinding (G), EDM (EDM), Sandblasting (SB), and 3D Printing (TP)

Table 9. Classification Experiment (with d=2)

Training							
M	**S**	**G**	**EDM**	**SB**	**TP**	**Accuracy**	**Classified as**
150						**100%**	M
	150					**100%**	S
		150				**100%**	G
			150			**100%**	EDM
				150		**100%**	SB
					150	**100%**	TP

Testing							
M	**S**	**G**	**EDM**	**SB**	**TP**	**Accuracy**	**Classified as**
143	**2**	**0**	**4**	**1**		**95.33%**	M
	142	**0**	**2**	**4**	**2**	**94.66%**	S
		143	**2**	**0**	**5**	**95.33%**	G
			144	**4**	**2**	**96%**	EDM
			1	**144**	**5**	**96%**	SB
				0	**150**	**100%**	TP

Note: Milling (M), Shaping (S), Grinding (G), EDM (EDM), Sandblasting (SB), and 3D Printing (TP)

Table 10. Classification Experiment (with d=3)

Training							
M	**S**	**G**	**EDM**	**SB**	**TP**	**Accuracy**	**Classified as**
150						**100%**	M
	150					**100%**	S
		150				**100%**	G
			150			**100%**	EDM
				150		**100%**	SB
					150	**100%**	TP

Testing							
M	**S**	**G**	**EDM**	**SB**	**TP**	**Accuracy**	**Classified as**
143	**2**	**0**	**4**	**1**		**95.33%**	M
	142	**0**	**2**	**4**	**2**	**94.66%**	S
		143	**2**	**0**	**5**	**95.33%**	G
			144	**4**	**2**	**96%**	EDM
			1	**144**	**5**	**96%**	SB
				0	**150**	**100%**	TP

Note: Milling (M), Shaping (S), Grinding (G), EDM (EDM), Sandblasting (SB), and 3D Printing (TP)

The classification experiment was performed using six types of specimens. The images were classed into training sets and test sets. Each training set and test set had 150 images. Initially, the software was trained using 150 images, as shown in Table 8, Table 9, and Table 10, respectively. Once the software is trained, the images from the test sets are used for classification. Table 8, Table 9, and Table 10 respectively show the classification accuracies of the software for various specimens. What is evident from the above experiment is that classification accuracy got improved when the distance increased from d= 1 to d=2. However, when the distance is increased from d=2 to d=3, an increase in the classification accuracy is not significant. Thus d=2 would give the best classification accuracy.

5. Conclusion

The current research has made an effort to perform texture analysis of machined and 3d printed surfaces. GLCM technique was used for extracting various textures. It was revealed from the experiment the texture values would depend on the distance and angle metrics used while computing the grey level co-occurrence matrix. The experimental investigation revealed that when distance =1, the classification accuracy was less. However, the classification accuracy improved when distance =2, but a further increase in the distance would not significantly improve the classification accuracy. Instead it would add up to the computational time. Thus, it was concluded that d=2 gave maximum classification accuracy of 96%.

References

Chang, T. and C. Kuo. Texture analysis and classification with tree-structured wavelet transform. IEEE Trans. Image Proc., 2(4):429–441, 1993.

Du, L. J., "Texture Segmentation of SAR Images Using Localized Spatial Filtering," In Proceedings of International Geoscience and Remote Sensing Symposium, pp. 1983-1986, Washington, DC, 1990.

Farrokhnia, F., Multi-channel filtering techniques for texture segmentation and surface quality inspection, Ph.D. thesis, Computer Science Department, Michigan State University, 1990.

Haralick, R.M., "Statistical and Structural Approaches to Texture," Proceedings of the IEEE, 67, pp. 786-804, 1979.

Julesz, B., E. N. Gilbert, L. A. Shepp, and H. L. Frisch, "Inability of humans to discriminate between visual textures that agree in second-order statistics - revisited," Perception, 2, pp.391-405,1973.

Jain, A.K. and F. Farrokhnia. "Unsupervised Texture Segmentation Using Gabor Filters," Pattern Recognition, 24, pp. 1167-1186, 1991.

Kiran, M.B., A novel online surface roughness measuring method, Proceedings of the International Conference on Industrial Engineering and Operations Management, 2021, pp. 2907–2916

Kiran, M. B., Automated Product Inspection in Industry 4.0 Environmen2021 IOP Conf. Ser.: Mater. Sci. Eng. 1146 012003

Kiran, M.B., B Ramamoorthy, V Radhakrishnan, Evaluation of surface roughness by the vision system, International journal of machine tools and manufacture 38 (5-6), 685-690,1998.

Ma, Y., and B. Manjunath. A comparison of wavelet transform features for texture image annotation. ICIP, 1995

Ohanian, P. and R. Dubes. Performance evaluation for four classes of textural features. Pattern Recognition, 25:819–833, 1992

Ojala, T. M. Pietikainen, and D. Harwood. A comparative study of texture measures with classification based on feature distribution. Pattern Recognition, 29:51–59, 1996.

Patel, D. R., Thakker, H., Kiran, M., & Vakharia, V., Surface roughness prediction of machined components using gray level co-occurrence matrix and Bagging Tree. FME Transactions, vol. 48,no.2, pp. 468-475, 2020.

Patel, Dr, Kiran, MB, Vakharia, V. Modeling and prediction of surface roughness using multiple regressions: A noncontact approach. Engineering Reports. 2020; 2:e12119. https://doi.org/10.1002/eng2.12119

Rignot, E. and R. Kwok, "Extraction of Textural Features in SAR Images: Statistical Model and Sensitivity," In Proceedings of International Geoscience and Remote Sensing Symposium, pp. 1979-1982, Washington, DC, 1990.

Reed, T., and J. Du Buf. A review of recent texture segmentation and feature extraction techniques. CVGIP, 57(3):359–373, 1993.

Smith, J. and S.-F. Chang. Transform features for texture classification and discrimination in large image databases., ICIP, 1994.

Van Gool, P. Dewaele, and A. Oosterlinck. Texture analysis. CVGIP, 29(3):336–357, 1985.

Schistad, A. H. and A. K. Jain, "Texture Analysis in the Presence of Speckle Noise," In Proceedings of IEEE Geoscience and Remote Sensing Symposium, Houston, TX, May 1992.

